

The Composite Channel Method: Efficient Experimental Evaluation of a Realistic MIMO Terminal in the Presence of a Human Body

Fredrik Harrysson^{*‡}, Jonas Medbo^{*}, Andreas F. Molisch^{†‡}, Anders J. Johansson[‡] and Fredrik Tufvesson[‡]

^{*}Ericsson Research, Ericsson AB, Sweden

[†]Mitsubishi Electric Research Laboratories (MERL), USA

[‡]Dept. of Electrical and Information Technology, Lund University, Sweden

Email: fredrik.harrysson@ericsson.com

Abstract—The immediate environment of the transmit (TX) and receive (RX) antennas, including the antenna casings and the users holding the antennas, has a strong impact on the propagation channel and thus on wireless systems. In this paper we experimentally evaluate a method that synthetically combines double-directional measurements of the propagation channel (without the user influence) with measured antenna patterns of antennas-plus-users, by comparing obtained sample results with direct measurements in the same environment. The measurements are done for a static microcell 8x4 MIMO scenario at 2.6 GHz. A realistic user phantom was used together with a test terminal prototype with four antenna elements, and a number of different configurations and orientations of the phantom were tested. In average over all test cases, the mean signal power deviation between composite channel method and measurements was well within 1 dB. The composite method shows 6% higher terminal antenna correlation but similar statistical distributions as the measured. The differences between the model and measurements for the strongest eigenvalue (relevant for MRC combining) was found to be within 1 dB above 10% outage level. Relative deviations in the ergodic MIMO capacity were smaller than 10%.

I. INTRODUCTION

In order to implement Multiple-Input Multiple-Output (MIMO) to its full potential in mobile communication systems, it is important to understand the impact of the user body and the antenna configurations in user equipments on the system performance. A full, realistic performance assessment would require extensive measurement campaigns in realistic operation environments, using the specific terminal antenna arrangement of interest, and different humans holding the device. However, such extensive measurement campaigns are cumbersome and expensive.

To avoid extensive measurement campaigns a composite measurement approach that combines a *single* measurement campaign for the double-directional propagation channel alone with a measurement of users and antenna characteristics in an anechoic chamber can be used. The double-directional impulse response is interpreted as a sum of contributions from multipath components (MPCs), which are in turn characterized by their directions-of-arrival and directions-of-departure, as well as their delays [1].

The composite measurement approach is based on two facts (i) the double-directional propagation channel describes

only the multipath propagation itself and is thus free of any influence of the antennas, and (ii) the user (including its head, hand, and torso) together with the actual handset (antennas as well as casing) can be interpreted as a "superantenna" that can be characterized by its antenna pattern and frequency dependence, and that weights and adds up the MPCs. Thus, a double-directional channel measurement can be combined with *any* measurement of the superantenna characteristic to describe the combined effect of channel, user, and antenna. This in particular allows a completely fair and reproducible comparison of different antenna arrangements in the chosen propagation environment. Several papers have used the principle of combining double-directional channel characterization with antenna radiation patterns. [2] used the method with simple antenna arrangements to generate multiple channel realizations; [3, 4] pioneered the combination of channel measurements with antenna patterns of realistic handset antenna configurations and compared the results to direct measurements; [5] used ray tracing and Method-of-Moment simulations in a similar fashion. However, previous publications have either completely ignored the presence of the user, or used very simplified models: only the impact of the head has been analyzed,¹ even though both theoretical and experimental investigations showed the importance of user hand and torso [6], [7], [8].

The goal of the present paper is to investigate whether the composite channel method can also appropriately account for the presence of realistic setups including full models of users. The novel contributions of the paper are thus the following:

- 1) we test the composite channel model with a body phantom that includes hand and upper torso as well as head.
- 2) we test the impact of different hand positions on the results.
- 3) we investigate the influence of different usage positions of the cellphone (i.e., holding it in PDA-type mode).
- 4) we analyze the MIMO capacity as well as eigenvalue distribution and diversity performance for four antennas on the test terminal in the presence of a user.

¹ the only composite-method investigation including the head [3] analyzes the performance of a 2x2 system; no larger arrangements are present



Fig. 1. The terminal with case open (compared to a common-size mobile phone) and the user phantom in the multimedia mode.

II. PRINCIPLE OF THE COMPOSITE METHOD

The main principle of the composite method is to combine a double-directional description of the wireless propagation channel with the antenna pattern of the superantenna. This provides the channel matrix $\mathbf{H}(f)$, whose elements $H_{ij}(f)$ describe the transfer function from the j -th transmit to the i -th receive antenna element.

In the composite method, the channel matrix is calculated by joining the double-directional channel description with the antenna pattern as

$$\mathbf{H}(f) = \sum_{l=1}^L \mathbf{A}_r^t(\Omega_{r,l}, f) \mathbf{P}_l(f) \mathbf{A}_t(\Omega_{t,l}, f) e^{-j2\pi f \tau_l} \quad (1)$$

Here L is the number of MPCs, τ_l , $\Omega_{r,l}$ and $\Omega_{t,l}$ are the delay, DoA and DoD for the l 'th ray, respectively, and \mathbf{P}_l is the complex 2×2 amplitude and polarization matrix for the l -th multipath component. The receive and transmit antenna matrices $\mathbf{A}_{r,t}$ contain the antenna gains and array steering vector phase term (inherent in the measured super-antenna patterns) for each element in the columns, and for the polarization component (θ, ϕ) in the rows, i.e. $n_{r,t} \times 2$.

The composite channel matrices can be compared to directly measured matrices as elaborated in Section IV.

III. TERMINAL AND USER PHANTOM

The handset used in the experiments is a PDA terminal mock-up with four antenna (PIFA) elements, see Fig. 1 (left). During both pattern and channel measurements, a semiconductor switch was used to select the active port while the others were terminated. The user phantom consist of two separate parts, a liquid² filled upper body phantom (torso and head) and a solid hand/lower arm phantom³.

A. User Modes

Three different phantom and terminal configurations were studied; talk mode ("tm"), multimedia mode with antenna side of handset downwards ("mm"), and multimedia mode with the antenna side upwards ("mmb"). *Talk mode* represents the scenario where the user holds the terminal in the right hand, toward the right ear, while *multimedia mode* represents the scenario where the user hold the terminal in the right hand as to watch the screen. The individual performance of the four

²Head tissue simulant liquid in compliance with IEEE Std. 1528 at 2.6 GHz, with $\epsilon_r = 39.7$ and $\sigma = 2.14$.

³Hand and lower arm piece from IndexSAR[©] (www.indexsar.com)

terminal antennas may differ significantly, depending on the position of the terminal with respect to the hand. Thus, in each mode, the terminal was placed at three positions with relative offset of 10 mm inside the hand.

B. Radiation Pattern Measurements

The full-sphere antenna patterns, including polarization, amplitude and phase, of the handset-phantom combination were measured at six frequencies in the range 2.5-2.7 GHz. We also tested whether the repeatability of the results was retained when the terminal was taken out of, and subsequently reinserted into, the hand after reconfiguration of the arm. The measurements were repeated for one user scenario and the pattern correlation, i.e. the normalized full-sphere integral vector product between two antenna patterns, were calculated. This was found to be on average 0.95 for one antenna element compared before and after reassembly. For two different antenna elements, i.e. pattern (cross-) correlation of two different elements, it was found to be 0.20 (independent of whether the antenna elements are compared before or after reassembly).

IV. PROPAGATION CHANNEL

A. Measurement Procedure

The channel measurements were performed at an office building of Ericsson AB in Kista, Sweden, in an outdoor-indoor micro-cellular scenario. Two separate frequency bands were chosen, 2530-2550 MHz and 2610-2690 MHz, due to the available spectrum licenses. The BS (base station) location was in a skywalk above the street between two neighboring houses, and the MS (mobile station) was positioned in a lab whose windows are oriented towards the street, see Fig. 2. To enable MIMO measurements, at the BS position, a linear robot was used to move a probe antenna to 8 positions separated by 4 cm. The antenna was a vertically polarized square patch antenna, with 9 dBi gain and about 60° beamwidth, and its pattern was measured in a similar fashion as described in Section III-B. At the MS, two setups were used to enable two different types of measurements:

- 1) Firstly, a virtual-array channel sounding measurement was performed to enable a double-directional characterization of the channel alone, using a 3D positioning robot and a dual-polarized square patch antenna (similar to the BS antenna) at the MS, see Fig. 3. The robot moved the antenna to form a synthetic square 8x8-array with 4 cm element distance, rotated in steps of 90° to four directions. The parameters of the MPCs were extracted from these measurements using the maximum likelihood (ML) estimation method described in [9]; up to 2910 MPCs were resolved. The impact of the antenna patterns of the probe antennas at the MS side was removed through appropriate calibration.⁴
- 2) Secondly, direct measurements of the transfer functions were done with the robot and probe antenna exchanged

⁴At the BS side, antenna gain remain present throughout the analysis, since it had no impact on the relative comparison of the different approaches.

by the (static) 4-antenna terminal and the user phantom⁵. In each setup, the phantom was rotated in steps of 90° to four directions. The SNR of the measurements was better than 50 dB. Observed time-variant components due to wind-swept trees was suppressed to -20 dB versus the stationary components, by averaging over 10 repeated measurements.



Fig. 2. Site map of measurements with the BS position and the MS (3D robot) position marked. A few example (typical) rays are drawn.

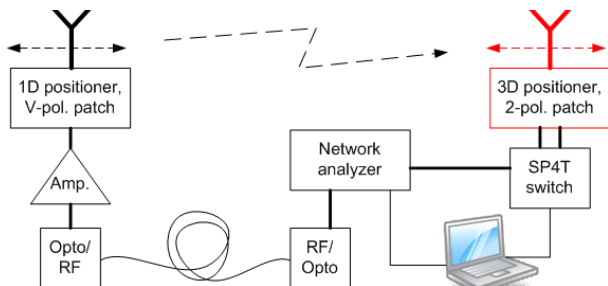


Fig. 3. Setup of channel characterization measurements with the 3D positioning robot and probe antenna at the Rx side. At the direct channel measurements the probe antenna was exchanged by the phantom and the 4-antenna terminal.

B. Double-Directional Characterization of the Channel

The double-directional channel characteristics are illustrated in Fig. 4. The relative MPC powers are represented by the size and the color of the circles. The plots show the corresponding angular and/or distance distributions. The strongest MPCs at the MS side are impinging from the windows towards the street, see Fig. 4a.

V. COMPARISON OF COMPOSITE AND DIRECT MEASUREMENTS

In this section, we compare the composite channel method (CM) to the direct measured (DM) channels for the MS scenarios with the different constellations of terminal and user phantom.

A. Mean Power

We first compare the mean received power at MS element i calculated as

$$P_i = \frac{1}{n_t} \sum_j^{n_t} |H_{ij}|^2 \quad (2)$$

⁵The robot fixture was present but not used for positioning

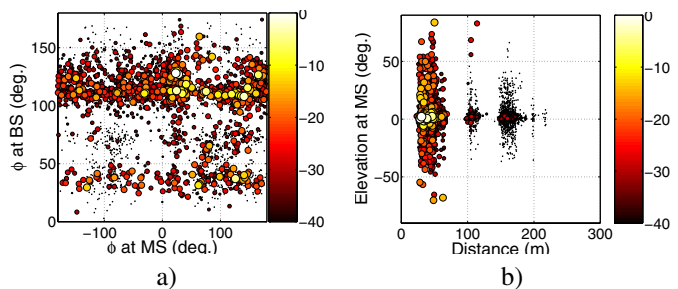


Fig. 4. Graphical presentation of the double-directional channel ray representation. The relative MPC power is represented by the size and the color of the circles (dB). The plots show examples of corresponding angular and distance distributions for a) BS azimuth vs. MS azimuth, and b) MS elevation vs. path distance .

and averaging over frequency. This implies that we assume frequency ergodicity, i.e., the frequency domain samples (together with the BS position samples) are treated as fast fading samples of narrow-band signals. In order to verify the extracted double-directional channel parameters, we start with comparing the results for the probe antenna at the MS. The composite method with 500 MPCs was found to give 85% of the measured power and the distribution showed excellent match, see Fig. 5.

For the measurements with the phantom, the results of the power comparison are shown in Fig. 6 where the power is averaged over frequency, BS elements and terminal-in-hand offsets. The abscissa represent indices of test configurations corresponding to the four MS antennas, the four user rotation angles, and the three user modes. The difference between the composite and the measured results is within 1 dB (which is estimated as the accuracy limit) in 15 of 48 test cases. The power gap between the power of the direct measurements and the composite channel matrices can mostly be attributed to limitations of the fundamental double-directional model (finite sum of plane waves) and has been observed in measurement campaigns in the literature. In some rare cases, the power in the composite channel is higher than in the directly measured channel. This is probably due to an insufficient number of samples, as well as other sources of inaccuracy. The maximum deviation is 5.5 dB (No. 3), the average difference 0.4 dB, difference in mean power 0.57 dB.

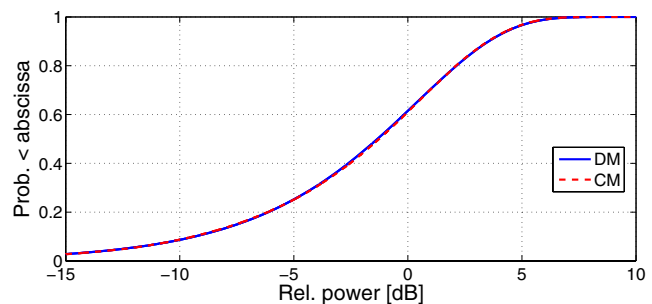


Fig. 5. Comparison of relative power distributions for the probe antenna directly measured (DM) and composite realization (CM). The power was normalized to the power average over frequency.

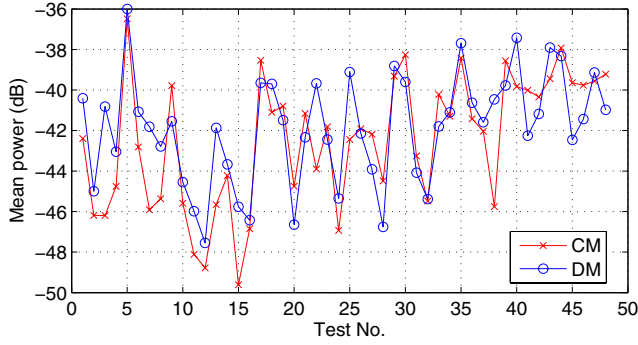


Fig. 6. Comparison of average receive power at the MS side for 48 test cases. The power was averaged over frequency, BS elements and terminal-in-hand offset.

Ant.	1	2	3	4
1	1	0.43/0.40	0.47/0.38	0.43/0.35
2		1	0.43/0.35	0.47/0.40
3			1	0.47/0.45
4				1

TABLE I
AVERAGE MAGNITUDES OF THE COMPLEX CORRELATION COEFFICIENTS FOR PAIR-WISE ANTENNA ELEMENTS (CM/DM).

B. Antenna Correlation

The antenna correlation coefficients ρ_{ij} at the receiver side was estimated from the sample covariance matrix with the proper normalization as

$$\mathbf{R} = \frac{1}{n_t n_f} \sum_{i=1}^{n_f} \mathbf{H}(f_i) \mathbf{H}^H(f_i) \quad (3)$$

$$\rho_{i,j} = \frac{R_{ij}}{\sqrt{R_{ii} R_{jj}}}$$

where n_f is the number of frequency samples. Thus, the sample space is the frequencies and the transmit antennas. To compare if the composite channel matrix show the same estimated MS antenna correlation as the directly measured one, the complex correlation coefficients are calculated according to (3). The average magnitude of complex coefficients for pairwise antenna elements is shown in Tab. I. The values show $|\rho_{i,j}|$ averaged over the terminal offsets, phantom rotations and user modes. The composite channel matrix gives 15% higher average correlation than the measured ones (0.45 vs. 0.39). The difference in correlation was quite large for different test cases. The 10 and 90 percentiles of the cumulative distribution over the test cases was around 0.2 and 0.6, respectively, but the difference between the composite and direct results at the 10 and 90-percentiles was below 0.1 for all antenna pairs (with one exception).

C. Eigenvalue Distribution

The distribution of the ordered eigenvalues is a key characteristic of MIMO systems. The strongest eigenvalue is a measure for the SNR that can be achieved by maximum-ratio transmission/maximum-ratio combining, while a weighted

sum of the logarithms of the eigenvalues characterizes the capacity of spatial-multiplexing systems.

The normalized eigenvalues are calculated for each 4x8 channel matrix as

$$\lambda^{(i)} = \frac{1}{\|\mathbf{H}^{(i)}\|_F^2} \text{eig} \left\{ \mathbf{H}^{(i)} \mathbf{H}^{(i)H} \right\} \quad (4)$$

where $\|\cdot\|_F^2$ is the squared Frobenius-norm. We consider the distribution of the eigenvalues over an ensemble containing all combinations of frequency, terminal offset and phantom user rotation. Fig. 7 shows the eigenvalue distribution of the composite and directly measured matrices for the three user modes. Additional curves show the distribution when additive white Gaussian noise (AWGN) to an SNR of 15 dB is included.⁶ Also, for comparison the distribution for an i.i.d. Rayleigh fading channel is plotted. AWGN does improve the agreement with direct measurements, but not for all eigenvalues simultaneously. Thus, the model inaccuracies are not following an i.i.d. AWGN model.⁷

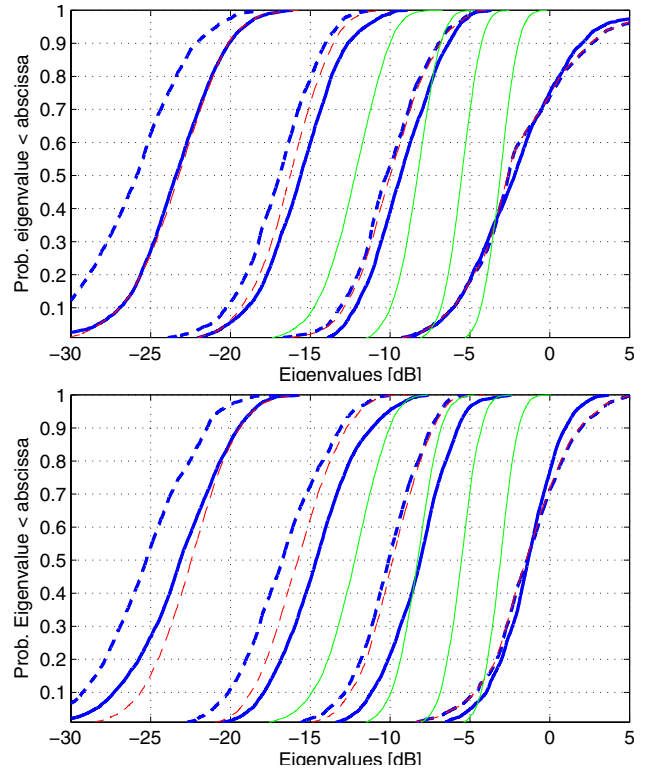


Fig. 7. Comparison of the eigenvalue distributions for talk mode "tm" (top) and multimedia mode "mm" (bottom), with DM case (solid), CM case (thick dashed), and CM+AWGN (thin dashed). For comparison, the distribution of i.i.d. Rayleigh fading is plotted (thin solid).

⁶The SNR is defined as signal power averaged over small-scale-fading realizations, i.e., averaged over the frequency samples; there is no averaging over terminal offsets or rotations.

⁷Part of the model inaccuracies stem from temporal variations due to wind-swept trees between the skywalk and the windows. The resulting time-variant contributions had an average power ratio of about -20 dB, but their impact is non-i.i.d., since the affected MPCs come only from a limited angular range.

D. Channel Capacity

An estimate of the information throughput potential, can be obtained by calculating the maximum mutual information. Following the concept of [10], we define the "instantaneous" capacity, with no channel information at the transmitter, as

$$C^{(i)} = \log_2 \det \left\{ \mathbf{I} + \frac{\rho}{n_t} \frac{\mathbf{H}^{(i)} \mathbf{H}^{(i)H}}{\frac{1}{n_t n_r} \|\mathbf{H}_{ref}^{(i)}\|_{F,slow}^2} \right\} \quad (5)$$

To ensure comparability of capacity performance of the different user modes, we use a common reference norm for the channel matrix in (5). This means that we investigate the case where slow fading (in this evaluation considered to be the phantom orientation and terminal-in-hand offset) is mitigated by system power control. The reference "slow fading" norm in (5) is calculated as the square Frobenius norm of each channel matrix sample, averaged over the three user modes and the 402 frequency samples⁸. The results for the ergodic (mean) capacity for a 4x8 system are shown in Fig. 8, for the three different user modes. There is a close agreement between the composite matrix results and the directly measured ones. The difference was found to be within 2.2 and 0.7 bits/s/Hz for SNRs below 20 dB or less than 19 and 10% at SNRs above 5 dB for a 4x8 and a 2x4 system, respectively (results for 2x4 not shown in the paper for space reasons).

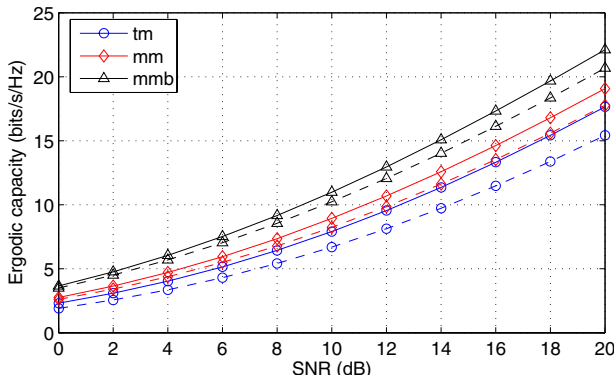


Fig. 8. Ergodic capacity vs. SNR for directly measured (solid) and composite (dashed) channel matrices.

VI. SUMMARY

We investigated the composite channel matrix approach for MIMO systems in the presence of user head, torso, and hand. In this approach a double-directional description of the wireless propagation channel is combined with antenna pattern measurements of user-plus-handset (superantenna). We evaluated the validity of the approach by comparisons with direct measurements. A realistic user phantom was used together with a realistic test terminal mock-up with four antenna elements, and a number of different configurations and orientations of the phantom was tested, such as user orientation, talk and multimedia (browsing) position, and terminal position in the phantom hand. It must be noted that the superantenna has much larger dimensions than a conventional handset, and thus

⁸Alternatively, a reference antenna can be used, as proposed in [11]

a larger Rayleigh (or Fraunhofer) distance. As a consequence, the vital assumption that all MPCs are originating from objects in the far-field might not always be fulfilled. The differences between the model and measurements for the strongest eigenvalue is within 1 dB above the 10% outage level; this is similar to other results presented in the literature. Not surprisingly, higher-order eigenvalues show a larger deviation between composite method and direct measurements; they can be up to 5 dB for the fourth eigenvalue. We found (details not presented here) that a application of the composite method to the channel with the probe antennas gave similar deviations from the direct measurements. A test adding white Gaussian noise did result in better agreement for certain eigenvalues depending on the SNR, but not all at the same time. Overall, we conclude that the composite approach is a highly valuable tool for the evaluation of multiple-antenna configurations in the presence of user head, torso, and hand. Even though the presence of the user body makes the comparison more difficult, we find that careful experimental design can overcome the problems.

ACKNOWLEDGMENT

The anechoic chamber measurements were performed at Sony-Ericsson Mobile Communications AB in Lund, Sweden. Part of this work was supported by an INGVAR grant of the Swedish SSF, and the SSF inter-university Center of Excellence for High-Speed Wireless Communications.

REFERENCES

- [1] M. Steinbauer, A. F. Molisch, and E. Bonek, "The double-directional radio channel," *IEEE Antennas Propagat. Mag.*, vol. 43, no. 4, pp. 51–63, 2001.
- [2] A. F. Molisch, M. Steinbauer, M. Toeltsch, E. Bonek, and R. Thoma, "Capacity of MIMO systems based on measured wireless channels," *IEEE J. Select. Areas Commun.*, vol. 20, no. 3, pp. 561–569, 2002.
- [3] P. Suvikunnas, K. Sulonen, J. Villanen, C. Icheln, J. Ollikainen, and P. Vainikainen, "Evaluation of performance of multi-antenna terminals using two approaches," in *IMTC 2004 – Instrum. and Meas. Technol. Conf.*, Como, Italy, 2004.
- [4] P. Suvikunnas, J. Villanen, K. Sulonen, C. Icheln, J. Ollikainen, and P. Vainikainen, "Evaluation of the performance of multiantenna terminals using a new approach," *IEEE Trans. Instrum. Meas.*, vol. 55, no. 5, pp. 1804–1813, 2006.
- [5] K. Dandekar and J. Heath, R.W., "Modelling realistic electromagnetic effects on MIMO system capacity," *IEE Electronics Letters*, vol. 38, no. 25, pp. 1624–1625, 2002.
- [6] A. Yamamoto, H. Toshiteru, O. Koichi, K. Olesen, J. O. Nielsen, N. Zheng, and G. F. Pedersen, "Comparison of phantoms for browsing position by a NLOS outdoor MIMO propagation test," in *Proceedings of ISAP2007*, Niigata, Japan, 2007, pp. 1342–1345.
- [7] P. Erätuuli and E. Bonek, "Diversity arrangements for internal handset antennas," in *IEEE International Symposium on Personal, Indoor and Mobile Radio Communications PIMRC*, vol. 2, 1997, pp. 589–593.
- [8] M. Pelosi, G. F. Pedersen, and M. B. Knudsen, "Influence of human hand on mobile phone radiation," COST 2100, Tech. Rep. TD (07)036, Febr. 2007.
- [9] J. Medbo, M. Riback, H. Asplund, and J. Berg, "MIMO channel characteristics in a small macrocell measured at 5.25 GHz and 200 MHz bandwidth," in *IEEE Veh. Technol. Conf. VTC*, vol. 1, 2005-Fall, pp. 372–376.
- [10] G.-J. Foschini and M.-J. Gans, "On limits of wireless communications in a fading environment when using multiple antennas," *Wireless Personal Communications*, vol. 6(3), pp. 311–35, 1998.
- [11] P. Suvikunnas, J. Salo, J. Kivinen, and P. Vainikainen, "Empirical comparison of MIMO antenna configurations," in *IEEE Veh. Technol. Conf. VTC*, 2005-Spring.